# Dispatched mediates Hedgehog basolateral release to form the long-range morphogenetic gradient in the *Drosophila* wing disk epithelium

**Ainhoa Callejo, Aphrodite Bilioni, Emanuela Mollica, Nicole Gorfinkiel, Germán Andrés, Carmen Ibáñez, Carlos Torroja, Laura Doglio, Javier Sierra, and Isabel Guerrero[1]**

Centro de Biología Molecular "Severo Ochoa" (CSIC-UAM), Universidad Autónoma de Madrid, Cantoblanco, E-28049 Madrid, Spain

This Feature Article is part of a series identified by the Editorial Board as reporting findings of exceptional significance.

Edited by Matthew P. Scott, Stanford University/Howard Hughes Medical Institute, Stanford, CA, and approved May 13, 2011 (received for review April 29, 2011)

**Hedgehog (Hh) moves from the producing cells to regulate the growth and development of distant cells in a variety of tissues. Here, we have investigated the mechanism of Hh release from the producing cells to form a morphogenetic gradient in the *Drosophila* wing imaginal disk epithelium. We describe that Hh reaches both apical and basolateral plasma membranes, but the apical Hh is subsequently internalized in the producing cells and routed to the basolateral surface, where Hh is released to form a long-range gradient. Functional analysis of the 12-transmembrane protein Dispatched, the glypican Dally-like (Dlp) protein, and the Ig-like and FNNIII domains of protein Interference Hh (Ihog) revealed that Dispatched could be involved in the regulation of vesicular trafficking necessary for basolateral release of Hh, Dlp, and Ihog. We also show that Dlp is needed in Hh-producing cells to allow for Hh release and that Ihog, which has been previously described as an Hh coreceptor, anchors Hh to the basolateral part of the disk epithelium.**

The Hedgehog (Hh) signaling pathway is crucial for the development of a wide range of organisms from *Drosophila* to humans. Hh signaling is also needed in adult stem cell maintenance (1), cell migration (2) and axon guidance (3). Alteration of Hh function during development causes a variety of congenital disorders, whereas aberrant activation of the pathway has been implicated in many types of human cancers (4).

Hh is able to signal both short and long range, and it acts as a morphogen during development in various systems (5). One of these paradigms, the *Drosophila* wing imaginal disk, is a flattened sac made of two layers of closely juxtaposed and polarized epithelial cells, the columnar cells of the "disk proper" and the squamous cells of the "peripodial membrane." Both epithelia have their apical surfaces oriented toward the disk lumen. In each of these single-layered epithelia, two populations of cells with different adhesion affinities divide the field into posterior (P) and anterior (A) compartments (6). The P compartment cells produce Hh, which moves across the A/P compartment border, decreasing in concentration as it spreads away from the border. Although the apical surfaces of both epithelia are in close proximity, the A/P border is not aligned and Hh disperses independently across each of them (reviewed in ref. 7). Related to this issue, an important and controversial question is in which part of the epithelium, apical vs. basolateral, the Hh gradient is formed.

The Hh protein is synthesized as a precursor that is activated by a series of posttranslational modifications. The mature protein has a palmitic acid covalently attached to the amino terminus and a cholesterol moiety attached to the carboxyl-terminus (8). These lipid adducts confer to Hh high affinity for cell membranes (9). Nevertheless, Hh can signal to cells distant from the source (5), suggesting the involvement of specific release mechanisms of this lipid-modified protein (9). It has been found that *dispatched* (*disp*) gene is required exclusively in Hh-producing cells for the release of a fully functional Hh protein (10, 11). In *disp* mutant wing disks, Hh synthesis and lipid modifications are unaffected, but Hh accumulates at the plasma membrane of producing cells; presumably as a consequence, signaling is limited to cells adjacent to the producing cells and long-range signaling is abolished (11).

The mechanism of Hh spreading is still highly controversial (7). Several models that implicate the extracellular matrix as a scaffold for transport have been proposed (reviewed in refs. 12 and 13). It has been reported that the interaction of heparan sulfate proteoglycans (HSPGs) with lipid-modified Hh restricts the free spreading of Hh (14, 15). Among the HSPGs, glypicans are bound to the cell membrane via a GPI anchor and are required for Hh spreading (16). Currently available evidence implicates the glypican Dally-like (Dlp) also in Hh reception, acting together with the Hh receptor Patched (Ptc) (17, 18). Ptc restricts Hh movement by promoting endocytosis and subsequent degradation of the Hh protein (19–21). It is also known that Ptc interacts with both Dlp and the Ig-like and FNNIII domain protein Interference Hh (Ihog) (22, 23). Recently, it has been reported that the activities of Ihog and the closely related Brother of Ihog (Boi) are absolutely required for presentation of Ptc on the cell surface (24) and for sequestration of the Hh protein to limit long-range signaling (25). Here, we have investigated whether Ihog and Dlp could also have a role in Hh release from the producing cells.

Hh is secreted from highly polarized cells in most of the systems, and it seems to be secreted by the apical and basolateral plasma membranes in the wing disk (14, 26, 27) in chick (28) and mouse (29) embryos. Although there are two pools of Hh, apical and basolateral in the wing disk epithelium, we show here that the Hh directed to the apical membrane is subsequently internalized before its final release at the basolateral surface, where the Hh gradient is formed. We have also analyzed the interaction of Disp, Dlp, and Ihog in this Hh route. We observed that the glypicans Dlp and Disp mediate this basolateral Hh release and that Ihog interacts with Disp and Dlp in this process and attaches Hh to the basolateral plasma membrane.

## Results

**Basolateral Release of Hh to Form the Morphogenetic Gradient.** In a WT wing disk, Hh is produced in the P compartment (30) and is

Author contributions: I.G. designed research; A.C., A.B., E.M., N.G., G.A., C.I., C.T., L.D., J.S., and I.G. performed research; A.C., N.G., and L.D. contributed new reagents/analytic tools; A.C., A.B., N.G., G.A., C.T., and I.G. analyzed data; and A.C., A.B., and I.G. wrote the paper.

The authors declare no conflict of interest.

This article is a PNAS Direct Submission.

See Commentary on page 12565.

[1]To whom correspondence should be addressed. E-mail: iguerrero@cbm.uam.es.

This article contains supporting information online at www.pnas.org/lookup/suppl/doi:10.1073/pnas.1106881108/-/DCSupplemental.

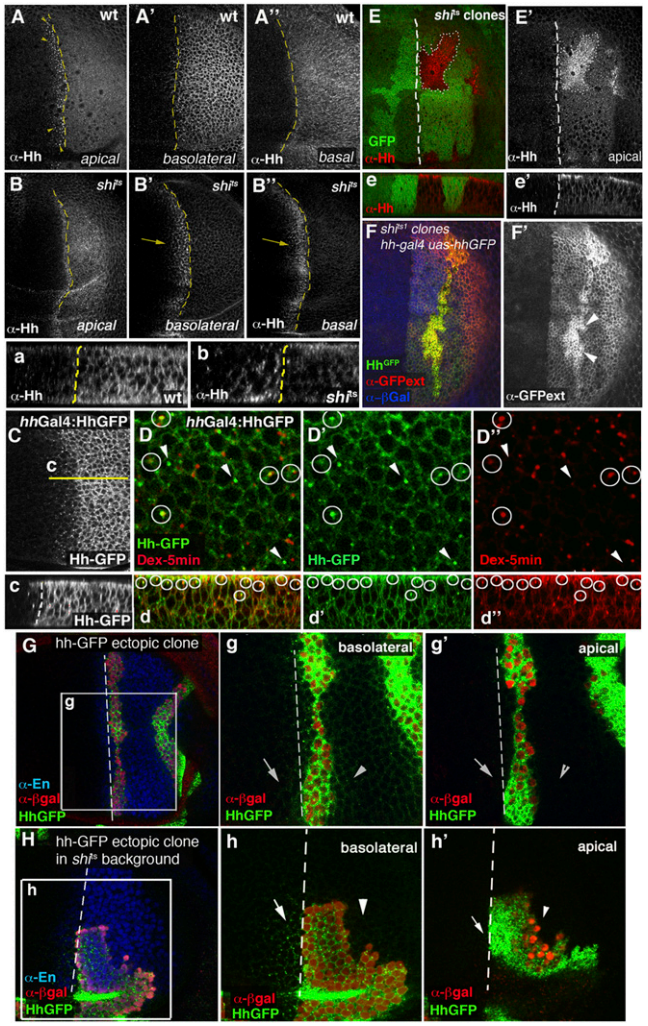


**Fig. 1.** Hh processing in the wing imaginal disk. Hh protein distribution in a WT imaginal disk (*A*–*A*′′) and in a *shi*$^{ts1}$ mutant disk after 2.5 h at the restricted temperature (*B*–*B*′′) in apical, lateral, and basal confocal sections. Note that Hh is present at similar levels in the apical and basolateral sections in a WT disk (transversal section *a*) in the P compartment and is also present in punctuated structures in the A compartment (arrowheads in *A*). (*B*) Note also the accumulation of Hh in the apical part of P cells and in the first row of A cells abutting the A/P compartment border in a *shi*$^{ts1}$ disk. In lateral and basal sections, Hh levels decrease in P cells, whereas Hh accumulates in several rows of the A compartment (arrow in *B*′ and *B*′′ and orthogonal view *b*). hh-Gal4/UAS-HhGFP wing imaginal disk (*C*) and transversal section of the same disk (*c*). (*D*–*D*′′) In vivo labeling by internalized red fluorescent dextran (5-min pulse) in an *hh*-Gal4/UAS-HhGFP wing disk. Circles indicate the colocalization of HhGFP with the internalized red fluorescent dextran, and arrowheads indicate the HhGFP vesicles that do not colocalize with the red fluorescent dextran. (*d*–*d*′′) Transversal section of the same wing disk to show the colocalization between Hh puncta and red fluorescent dextran. (*E* and *E*′) Accumulation of Hh (red) in *shi*$^{ts1}$ clones (lack of green). (*e* and *e*′) Apical Hh accumulation in *shi*$^{ts1}$ clones is shown in a transversal section of the same disk. (*F* and *F*′) Extracellular staining using an anti-GFP antibody in *shi*$^{ts1}$ clones in an *hh*-Gal4/UAS-HhGFP wing disk. Observe the extracellular apical accumulation of GFP (red in *F* and gray in *F*′) in *shi*$^{ts1}$ clones. (*G* and *Insets g* and *g*′) Ectopic HhGFP clone (marked in red by βGal staining) in the P compartment labeled by En expression (blue). Observe the basolateral and not the apical spreading of the HhGFP gradient outside the clone in the P (arrowheads). (*H*) Ectopic HhGFP clones in a *shi*$^{ts}$ background stained with anti-βGal (red) and anti-En (blue) antibodies. Dynamin-mediated apical internalization of Hh is observed in the P ectopic clone cells only (*Inset h*′) and not in the adjacent A clone, where dynamin-mediated internalization takes place through the basolateral plasma membrane (*Inset h*, arrow). Note also that the basolateral spreading of HhGFP outside the clone in the P compartment, shown in *Inset g*, is not observed in *Inset h*, indicating that when there is "freezing" internalization, there is less Hh at the basolateral plane (arrowhead) and that apical internalization of Hh is needed for the formation of a basolateral Hh gradient. In all transversal sections, the apical part of disks is in the upper part of the panels.

also detected in A compartment cells near the A/P border in internalized vesicles (Fig. 1*A*, arrowheads) (21, 30). In the Hh-producing cells, a large amount of Hh is observed in both the apical and basolateral plasma membranes, indicating that Hh is probably secreted through both surfaces (Fig. 1 *A*–*A*′′ and transversal plane *a*). To see in which part of the disk epithelium, apical vs. basolateral, the secreted Hh is internalized in the receiving cells to form the gradient, we used "freezing" endocytosis with a temperature-sensitive Dynamin mutant (*shi*$^{ts1}$), which blocks separation of endocytic vesicles from the parental membranes (31). By using freezing endocytosis for a short period in *shi*$^{ts1}$ disks, we observed that Hh accumulated basolaterally in the A compartment in a stripe of 5- to 10-cell diameters that strikingly corresponds to the extension of the Hh gradient (Fig. 1 *B*′ and *B*′′, arrows, and orthogonal view *b*). However, at a more apical optical section, Hh accumulated only in A cells touching the A/P border (Fig. 1*B*). Significantly, the Hh receptor Ptc accumulates both apically and basolaterally in *shi*$^{ts1}$ disks (Fig. S1 *B*–*B*′′ and *A*–*A*′′ for WT) or by expressing a dominant-negative form of Shi (Shi$^{DN}$) (32) in the A compartment (Fig. S1 *C*–*C*′′), but it colocalizes with Hh at the basolateral sections (Fig. S1 *B*′, *B*′′, *C*′, and *C*′′). This result indicates that Ptc probably recycles through all cell membranes but interacts with Hh through the basolateral membranes. This pattern of Hh and Ptc colocalization at the basolateral plane, once internalization is blocked, strongly suggests that the "long-range" Hh gradient is formed on this side of the disk epithelium.

**Hh Undergoes Endocytosis in Producing Cells.** In *shi*$^{ts1}$ disks, we also noticed that Hh accumulated at the apical surface of the epithelium in the P compartment cells, indicating that the apical secreted Hh is probably internalized in the same producing cells. Using an antibody against Hh, or looking at an HhGFP construct expressed in the P compartment, we detected Hh not only at the apical and basolateral plasma membranes but in discrete puncta (Fig. 1*C* and orthogonal view *c*). Some of these puncta could be labeled by internalized red fluorescent dextran, suggesting that they correspond to endocytic vesicles (Fig. 1 *D*–*D*′′ circles and orthogonal views *d*–*d*′′). To investigate the significance of this finding, we disrupted endocytosis in various genetic backgrounds and assessed the mechanism of Hh release.

As in *shi*$^{ts1}$ disks, *shi*$^{ts1}$ clones in the P compartment Hh accumulated at the apical surface of the epithelium (Fig. 1 *E* and *E*′ and orthogonal views *e* and *e*′). By extracellular staining using anti-GFP antibody containing *shi*$^{ts1}$ clones in an *hh*-Gal4/upstream activation sequence (UAS)-HhGFP disk, we observed that this Hh accumulation was extracellular (Fig. 1 *F* and *F*′). To investigate the effect of blocking internalization in Hh spreading further, we induced clones of HhGFP in the P compartment in both a normal and *shi*$^{ts1}$ background. Hh spreads away from an HhGFP clone induced in a WT disk at the basolateral surface (Fig. 1*G*, *Insets g* and *g*′, arrowheads). In *shi*$^{ts1}$ disks, however, HhGFP in the P compartment was limited in the expressing cells, where it accumulated apically. Meanwhile, it accumulated basolaterally in the A compartment as a result of Hh internalization in the receiving cells (Fig. 1*H*, *Insets h* and *h*′, arrows). We then decided to examine Hh distribution in disks expressing a dominant-negative form of Rab5 GTPase (Rab5$^{DN}$-YFP) that blocks early endosome formation (33). We observed that Hh also accumulated apically in cells expressing Rab5$^{DN}$-YFP (34) (Fig. 2 *A* and *A*′, arrowheads), whereas it decreased at the lateral side

(Fig. 2 *B* and *B′*, arrowheads). Together, these results suggest that Hh is targeted to the apical membrane and is subsequently internalized by Shi- and Rab5-mediated endocytosis. Because the cells that produce Hh also internalize it, we believe that apically localized Hh is not actually spreading but remains associated with the producing cell before endocytosis.

We further examined the process of Hh trafficking in P compartment cells by investigating whether Hh that is internalized from the apical surface is subsequently targeted to lysosomal degradation. Because *deep orange* (*dor*) mutants block transit of internalized cargo from the late endosomal compartment to lysosomes (35), we made clones of *dor* mutant cells and monitored Hh distribution. We observed that Hh levels in the P compartment clones were not much affected (Fig. S2 *A* and *A′*, clone 2), whereas in the A compartment, where Ptc has been shown to internalize Hh for lysosomal degradation (21), Hh accumulated much more in *dor* mutant cells (Fig. S2 *A* and *A′*, clone 1). These results suggest that in the P compartment, internalized Hh is not primarily targeted to degradation but is instead "recycled" (i.e., redirected to another part of the cell membrane for its final secretion). To test this hypothesis, we expressed a dominant-negative form of Rab8 and Rab4 proteins. Rab8 has been implicated in exocytic/recycling membrane trafficking during cholesterol removal from the endocytic circuits (36, 37). Because Hh could behave as a lipid molecule, we tested if knocking down Rab8 could affect Hh trafficking. Interestingly, after ectopic expression of dominant-negative Rab8 (34), Hh accumulated subapically (Fig. S2 *B* and *B′*, arrowheads), where the recycling endosome compartment is probably located (38). Vertebrate Rab4 directs rapid recycling from early endosomes to the plasma membrane (39, 40). We also observed a slight buildup of Hh protein in the apical part of the epithelium when we overexpressed a dominant-negative form of Rab4 (Fig. S2 *C* and *C′*, arrowheads).

Based on the above, we propose that in producing cells, the apical "secreted" Hh undergoes a subsequent endocytic internalization mediated by dynamin and Rab5 that leads to its "recycling" to the basolateral domain of the plasma membrane, where we believe the long-range Hh gradient is formed and shaped. In support of this hypothesis, when either $Rab5^{DN}$ or $Shi^{DN}$ was expressed in the whole P compartment, Hh signaling was compromised. The expression of the Hh targets Collier (Col) (41) and Ptc were reduced (from 7- to 4-cell diameters; Table S1) in both mutant conditions (Fig. 2 *C*, *C′*, *D*, *D′*, *F*, and *F′* compared with Col and Ptc WT expression in Fig. 2 *E* and *G*). Interestingly, we also noticed that by expressing $Shi^{DN}$ but not $Rab5^{DN}$, the long-range targets Cubitus interruptus (Ci) and Decapentaplegic (Dpp) were expanded (from 12- to 16-cell diameters) (Table S1 and Fig. 2 *C*, *C′*, *F*, *F″*, and *F‴* compared with Ci and Dpp WT expression in Fig. 2 *H* and *I*). Thus, by blocking internalization in the P compartment using $Shi^{DN}$, Hh most likely accumulates apically; this excess of Hh reaches the A compartment cells, activating only those targets that require low Hh levels, but is insufficient to activate the high-threshold Hh targets. In agreement with our results, an increase in apical Hh levels has been reported recently when internalization was blocked in the P compartment, causing activation of the low-threshold Hh targets as a result of a compensating phenomenon in which Hh is forced to signal improperly apically (27). Similarly, apical Hh internalization, able to activate the low-threshold Hh responses, has already been described by expressing a mutant Hh lacking cholesterol (Hh-N) in the P compartment (14). Collectively, these data indicate that after apical secretion, Hh has to be recycled to other membrane places; when this process is disturbed, the gradient is compromised.

**Disp Is Required for Hh Release Through the Basolateral Plasma Membrane.** In an attempt to analyze how Hh is released to reach the target A cells, we examined the role of Disp, the only protein shown to be required in producing cells for Hh release so far. As previously reported, Hh accumulates in *disp* mutant cells (11) (Fig. S3 *A* and *A′* and orthogonal views *a* and *a′*), but mutant forms of Hh that lacked lipid modifications, either Hh-N or palmitic acid (Hh-C85S) tagged to GFP, did not accumulate in

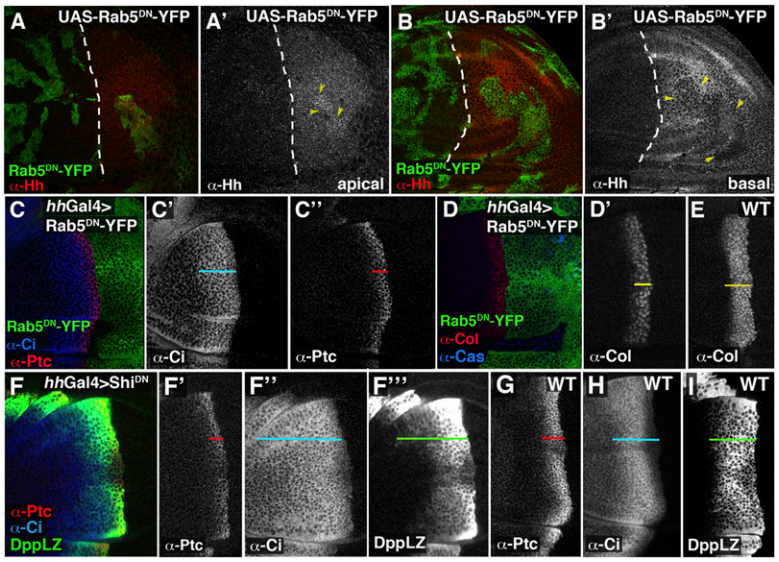


**Fig. 2.** Hh trafficking effects on gradient formation. (*A*–*B′*) Ectopic expression of $Rab5^{DN}$-YFP in clones (green) using the Tub-$Gal80^{ts}$ system after 30 h at the restrictive temperature. Observe that Hh accumulates apically (red in *A* and gray in *A′*, arrowheads) and decreases in the basal part of the epithelium (red in *B* and gray in *B′*, arrowheads). (*C*–*D′*) Tub-$Gal80^{ts}$; *hh*-Gal4/$Rab5^{DN}$-YFP wing disk after 33 h at the restrictive temperature. Although $Rab5^{DN}$-YFP does not cause activation of the apoptotic marker Caspase 3 (blue in *D*), it does provoke a decrease in Hh signaling as reported by the expression of $Ci^{155}$ (blue in *C* and gray in *C′*), Ptc (red in *C* and gray in *C″*), and Col (red in *D* and gray in *D′*). (*E*) Col expression in a WT disk. (*F*–*F‴*) Tub-$Gal80^{ts}$; *hh*-Gal4/$Shi^{DN}$ wing disk after 24 h at the restrictive temperature. Note that Ptc expression is reduced (*F′*) but Ci (*F″*) and Dpp (*F‴*) expression domains are expanded compared with WT expression of Ptc (*G*), Ci (*H*), and Dpp (*I*).

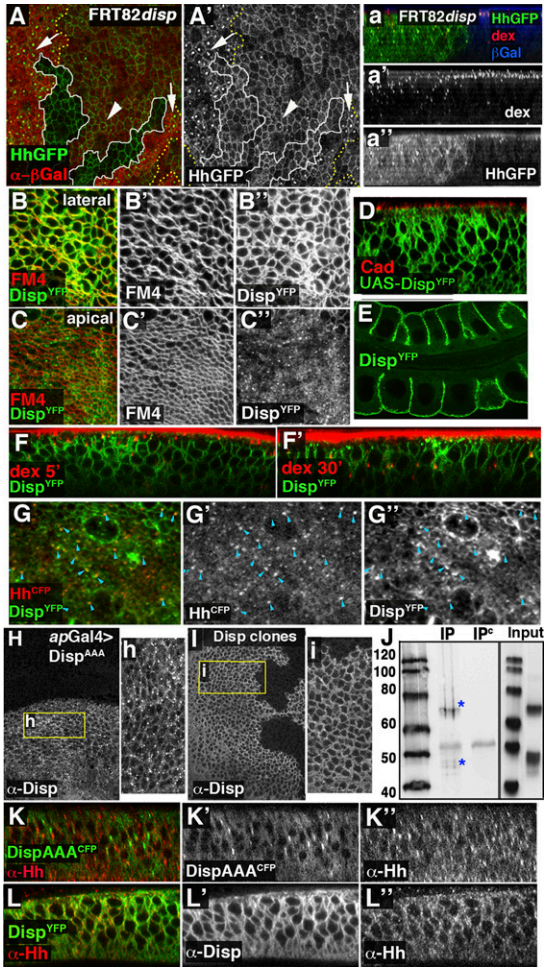


**Fig. 3.** Disp subcellular distribution and trafficking effects. (*A* and *A′*) *disp*$^{-/-}$ clones (lack of red) induced in an *en*-Gal4/UAS-HhGFP wing disk in a subapical view. Note the alteration in the subcellular distribution of apical Hh-GFP containing vesicles in *disp* mutant clones compared with twin clones (arrows in *A* and *A′*). (*a*–*a′′*) Transversal sections of a *disp*$^{-/-}$ clone induced in an *en*-Gal4/UAS-HhGFP wing disk (lack of blue) and in vivo labeled with red fluorescent dextran. Note the increase in Hh levels within the clone and in endocytic vesicles which colocalized with red fluorescent dextran puncta. Lateral (*B*–*B′′*) and apical (*C*–*C′′*) sections of an *hh*-Gal4/UAS-DispYFP wing disk stained in vivo with the membrane dye FM4 (red). Note that Disp colocalizes with the FM4 at the lateral (*B*–*B′′*) but not the apical (*C*–*C′′*) plasma membranes. (*D*) Transversal section of an *hh*-Gal4/UAS-DispYFP wing disk stained with an anti-Cadherin antibody (red) to label the subapical cell junctions. Note that Disp is localized at basolateral plasma membranes. (*E*) Salivary gland expressing DispYFP, which localizes at the basolateral plasma membrane and is excluded from apical membranes (*F* and *F′*). Transversal section of an *hh*-Gal4/UAS-DispYFP wing disk is stained with fluorescent red fluorescent dextran at a 5-min pulse (*F*) and a 30-min pulse (*F′*). Note that DispYFP and red fluorescent dextran colocalize in apically located vesicles after a short incubation (early endosomes) (*F*) and also in laterally located vesicles after a longer incubation (*F′*). (*G*–*G′′*) Wing imaginal disk expressing DispYFP and HhCFP (artificially labeled in red). Note the colocalization of Hh and Disp in some apical vesicles (blue arrowheads). (*H* and *I*) Wing disks expressing either a Disp$^{AAA}$ mutant construct in the dorsal compartment (*Inset h*) or random ectopic clones of the wild-type Disp protein (*Inset i*). Observe the distinct subcellular distribution of Disp$^{AAA}$ (*H* and *h*) and WT Disp (*I* and *i*); Disp$^{AAA}$ is less represented at the plasma membrane and is enriched in puncta (*K′* and *Inset h*). (*J*) Immunoprecipitation (IP) of Hh using a specific anti-Disp antibody. IP was carried out in extracts from salivary glands overexpressing Disp and HhGFP and was tested with an anti-Disp antibody. IP control was made from salivary glands overexpressing both HhGFP and Disp and tested with the preimmune serum. IP$^{c}$, IP control. Anti-GFP antibody was used in the Western blot. Note that the 70- and 47-kDa bands (asterisks), not present in the control, correspond to unprocessed and processed Hh, respectively, and that immunoglobulins (50-kDa) are present both in the IP and in the control. (*K* and *K′*) Transversal section of wing imaginal disk expressing Disp$^{AAA}$-CFP (artificially labeled in green) with *hh*Gal4 driver and stained with anti-Hh antibody. Note that there is not a significant colocalization between Hh and this Disp mutant form. (*L*–*L′′*) Transversal section of wing imaginal disk expressing DispYFP (artificially labeled in green) with *hh*-Gal4 driver and stained with anti-Hh antibody. Note the colocalization between Hh and DispYFP.

*disp*$^{-/-}$ clones (11) (Fig. S3 *C*–*D′*) and are freely released (Fig. S3*E*). It has also been described that Hh cannot signal in *disp*$^{-/-}$ disks (Fig. S3*F*, orthogonal planes *f* and *f′*). However, by overexpressing HhGFP in the P compartment of a *disp*$^{-/-}$ disk, a minor rescue of Hh signaling in cells touching the A/P compartment border could be provided (Fig. S3*G*, transversal planes *g* and *g′*). These data indicate that long-range signaling but not juxtacrine signaling requires *disp* function, as has been described previously in both *Drosophila* and vertebrates (42, 43). In P compartment cells lacking *disp* function, Hh levels increase in cell membranes (11) (Fig. S3 *A* and *A′* and orthogonal sections *a* and *a′*). The effect is cell-autonomous, and extracellular Hh labeling reveals that Hh accumulation in *disp* mutant clones takes place, at least in part, at the external face of the plasma membrane (Fig. S3 *B*–*B′′*). An apical section of a wing disk containing *disp* mutant clones indicates that Hh-puncta are also affected. More precisely, these puncta are mislocalized in the *disp*$^{-/-}$ clone, and also noticed in heterozygous *disp*$^{+/-}$ cells, compared with the WT territory (arrows for WT and arrowhead for twin clone in Fig. 3 *A* and *A′*). These puncta could be labeled by internalized red fluorescent dextran (Fig. 3, orthogonal views *a*–*a′′*), and are therefore likely to be endocytic vesicles. They increase in number, and although they are predominantly subapical in WT cells, they are randomly distributed in *disp* mutant cells compared with the WT territory (Fig. 3 *A* and *A′* and orthogonal views *a*–*a′′*). Because localization of most dextran-labeled vesicles, and not just the Hh-containing ones, changed in mutant cells, the role of *disp* might not be specific to Hh but more general in regulating vesicular trafficking. Therefore, we can propose a possible role of *disp* in the regulation of the intracellular trafficking of Hh (and perhaps other proteins) to the appropriate cell surface.

We also studied the subcellular localization of Disp protein using a DispYFP construct and specific α-Disp antibodies. Although Hh accumulates at the cell membranes in *disp* mutant cells, we observed that DispYFP was present mainly at the basolateral plasma membrane both in the imaginal disk (Fig. 3 *B*–*B′′* and *D*) and in salivary gland cells (Fig. 3*E*). Indeed, DispYFP was excluded from the apical plasma membrane, an arrangement that was clearly evident when the plasma membranes were labeled with the membrane dye FM4 (Fig. 3 *C*–*C′′*). Although absent from the apical membrane, DispYFP was clearly present in a group of subapical vesicles (Fig. 3*C′′*). DispYFP puncta could be labeled by internalized red fluorescent dextran, indicating that Disp is found in endocytic vesicles (Fig. 3 *F* and *F′*). Interestingly, after shorter times of incubation, the colocalization of Disp and dextran-labeled vesicles took place at more apical planes (Fig. 3*F*), whereas after longer incubation periods, the colocalization was evident at more basal domains (Fig. 3*F′*). This suggests that Disp traffics through different type of endosomes. In addition, by expressing both DispYFP and HhCFP, we observed that Disp puncta colocalized with some of the Hh puncta (~80% of colocalization) (blue arrowheads in Fig. 3 *G*–*G′′*). However, although Hh accumulated apically in *shi*$^{ts1}$ mutant clones, we did not detect any Disp accumulation at the plasma membrane of *shi*$^{ts1}$ cells (Fig. S3 *H* and *H′*, asterisk) or in the ectopic expression of Shi$^{DN}$ (Fig. S3 *I* and *I′*, asterisk), indicating that in contrast to Hh, the presence of Disp in these vesicles is not attributable to Disp in-

ternalization. Therefore, these vesicles could be either recycling endosomes or multivesicular bodies (MVBs), and they could define the endocytic compartment where Hh and Disp possibly meet.

The potential relevance of the colocalization of Disp and Hh in vesicles is enhanced by the additional finding that Hh and Disp can coimmunoprecipitate using anti-Disp–specific antibodies (Fig. 3*J*, asterisks). This result suggests that these proteins might interact directly. Because Hh is not released from *disp* mutant cells (11, 44) and accumulates in both the plasma membrane and intracellular vesicles, the role of Disp in vesicular trafficking may be consist in "capturing" Hh from apical endosomes and directing it to the basolateral surface.

It has been described that mutant forms of Disp in the GxxxD motif, in the transmembrane domains TM4 and TM10, lose the ability to release Hh protein in S2 cells (44). We tested one of these mutant forms of Disp ($Disp^{AAA}$) in the wing imaginal disk. We also observed a distinct subcellular distribution of $Disp^{AAA}$ (Fig. 3*H*, *Inset h*) compared with the WT protein (Fig. 3*I*, *Inset i*): a decreased distribution in the plasma membrane and, at the same time, an increase in the number of $Disp^{AAA}$-labeled vesicles. In addition, these $Disp^{AAA}$ vesicles do not colocalize with Hh puncta (Fig. 3*K* and *K′*) compared with the colocalization of Hh and Disp (Fig. 3 *L* and *L′*), implying that $Disp^{AAA}$ has an impaired the ability to participate in Hh vesicular trafficking to the basolateral plasma membrane.

**Dlp Is Needed for Optimal Hh Release.** Work from different laboratories has shown that Dlp interacts with Ptc (17) and Ihog (23) and that this interaction is necessary for Hh internalization in receiving cells. In contrast to previous reports (15, 45), we found that Hh protein levels in the P compartment of $dlp^{MH20}$ homozygous mutant disks were about 40% higher than in WT disks (Fig. 4 *A*–*C*). Examination of $dlp^{MH20}$ clones induced in the P compartment revealed that Hh protein levels in both apical (Fig. 4 *D* and *D′*) and basolateral (Fig. 4*E*, *Inset e*) membranes were consistently higher in *dlp* mutant cells compared with WT tissue.

Accumulation of Hh in a $dlp^{MH20}$ background suggests that in the absence of Dlp function, Hh release from producing cells might be impaired. Consistent with this hypothesis, when Dlp expression was knocked down by RNAi expression (Fig. S4 *C*, *C′*, and *Inset c′*) in the P compartment, Hh signaling was reduced, as monitored by the expression of Ptc, an Hh pathway target that is up-regulated at the compartment border (Fig. 4 *F*–*H*). Furthermore, we noted that the increase in Hh levels in P compartment $dlp^{MH20}$ clones was not uniform and that Hh levels did not increase in mutant cells found in close proximity to the clone borders (1- to 2-cell diameters; Fig. 4*e*, arrowheads). Based on the above, we conclude that Dlp has an important and previously uncharacterized role in Hh release from producing cells.

The similar pattern of Hh accumulation in plasma membranes of *disp* and *dlp* mutant cells made us analyze whether Dlp and Disp can interact. Indeed, Disp colocalizes with Dlp (Fig. 4*K*). Furthermore, overexpression of Disp increases Dlp levels at the basolateral plane of the epithelium (Fig. 4 *J*–*K′*). Given these findings, we also tested whether Disp and Dlp could biochemically interact. Using a specific anti-Disp antibody, we found that Disp and Dlp coimmunoprecipitate (Fig. 4*I*, asterisk). These data suggest that Disp interacts with Dlp in the process of Hh release from producing cells, and given the role of Disp in vesicular trafficking, we believe that Disp may also regulate the transcytosis of Dlp from the apical to basolateral plasma membrane. In agreement with the above, when a mutant form $Disp^{AAA}$ is ectopically expressed, it neither colocalizes nor accumulates Dlp as does WT Disp (Fig. 4 *L*–*M′*).

**Ihog Attaches Extracellular Hh to the Basolateral Part of the Disk Epithelium.** It has been characterized that *Drosophila* Ihog interacts directly with Dlp, Hh, and Ptc in the A compartment, where it functions during Hh reception (23, 24). Because Ihog is expressed throughout the wing disk (Fig. S4*D*) and interacts with Dlp during reception (23), we investigated whether Ihog also interacts with Dlp and Disp during Hh release from producing cells.

We first examined the localization of an IhogYFP fusion protein in randomly induced clones in the wing disk. We observed that IhogYFP localizes mainly at the basolateral plasma membranes and puncta, and also, interestingly, in long thin processes that extend away from cell borders (Fig. S5). We observed that ectopic Ihog expression increased Hh levels only at the basolateral plasma membrane (Fig. 5 *A*, *A′*, and *a*). Focusing at the basal part of the disk, we show that Hh was retained all along filopodia-like structures (Fig. 5*a′*, *Inset*) and that this accumulation was mainly extracellular (Fig. 5 *B*–*C′*). These data suggest

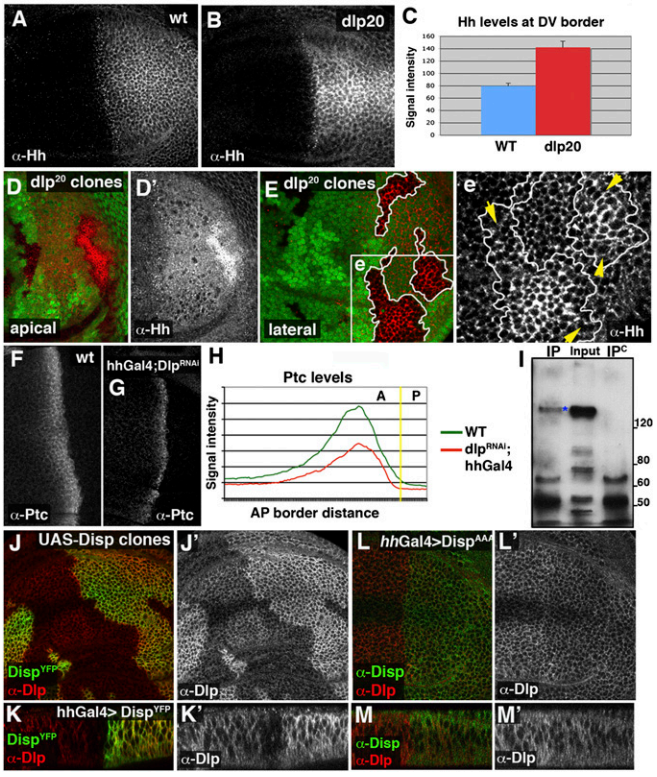


**Fig. 4.** Hh accumulation in the P compartment of *dlp* mutants. (*A*) Hh levels in a WT wing disk. (*B*) Hh levels in a $dlp^{MH20}$ null mutant wing disk. (*C*) Graph representing Hh levels in WT wing disks and in $dlp^{MH20}$ homozygous wing disks (average of equivalent areas of 6 disks, error bars represent SDs). (*D*–*E*) Hh levels in $dlp^{-/-}$ clones: an apical view is shown in *D′*, and a lateral view of another clone is shown in *E*. Hh accumulates at the cell membranes of $dlp^{MH20}$ mutant cells. (*Inset e*) Nonautonomous rescue in the mutant cells located near the clone border (arrowheads), which is also seen in *D*. (*F*) Ptc expression in a WT wing disk. (*G*) Ptc expression in an *hh*-Gal/UAS-$Dlp^{RNAi}$, Tub-$Gal80^{ts}$ disk after 30 h at the restrictive temperature. (*H*) Graph representing Ptc levels in WT wing disks and in an *hh*-Gal4/UAS-$Dlp^{RNAi}$ (average of expression levels of 6 disks). Observe the clear decrease of Ptc expression in *hh*-Gal4/UAS-$Dlp^{RNAi}$ disks. (*I*) Disp and Dlp co-immunoprecipitation (co-IP) using a specific anti-Disp antibody. The IP was performed in extracts from salivary glands overexpressing Disp and Dlp-GFP and tested with an anti-Disp antibody. IP control was made in extracts from salivary glands overexpressing only DlpGFP and tested with the same anti-Disp antibody. $IP^{c}$, IP control. Anti-GFP antibody was used in the Western blot [$Dlp^{GFP}$, 112 kDa (asterisk), and immunoglobulins, 50 kDa]. (*J* and *J′*) Dlp expression (red) in ectopic UAS-DispYFP clones. (*K* and *K′*) Transversal section of an *hh*-Gal4/UAS-DispYFP wing imaginal disk. Note that Dlp is up-regulated in ectopic Disp clones. (*L* and *L′*) Dlp expression (red) in ectopic UAS-$Disp^{AAA}$ using *hh*-Gal4 driver. (*M* and *M′*) Transversal section of the same disk. Observe that $Disp^{AAA}$-expressing cells do not accumulate Dlp.

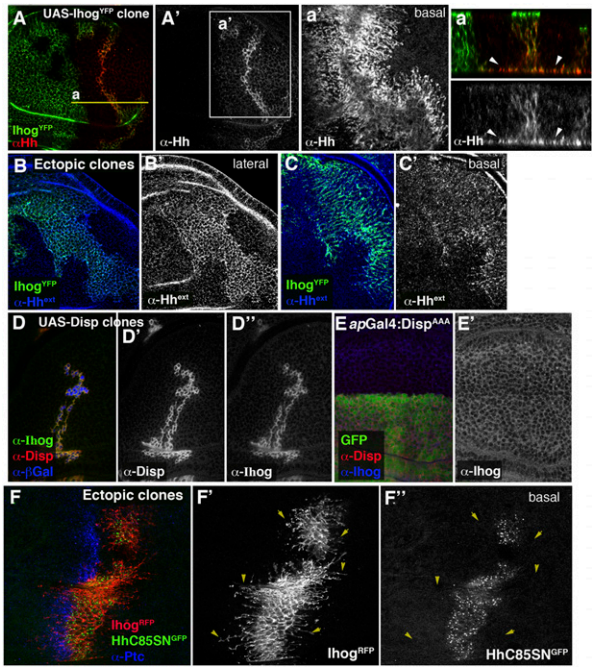


**Fig. 5.** Ihog attaches Hh basolaterally. (*A* and *A′*) Wing disk expressing IhogYFP for 24 h using the Gal80$^{ts}$ system stained with an anti-Hh antibody. Note that Hh levels increase in the clones. (*Inset a′*) Basal view of the IhogYFP clone shown in *A*. Note that Hh accumulation extends several cell diameters at the most basal part of the epithelium. (*a*) Transversal section of an ectopic IhogYFP clone (yellow line in *A*). (*B–C′*) Extracellular Hh staining using an anti-Hh antibody in ectopic IhogYFP clones. Note the cell surface accumulation of Hh in lateral (*B* and *B′*) and basal (*C* and *C′*) confocal sections. (*D–D′′*) Ectopic Disp clones marked by anti-βGal staining (blue in *D*) and by the specific anti-Disp antibody (red in *D* and gray in *D′*) increase endogenous Ihog levels (green in *D* and gray in *D′′*). (*E* and *E′*) Wing disk expressing Disp$^{AAA}$ in the dorsal compartment for 44 h using *ap*-Gal4; Tub-Gal80$^{ts}$ driver marked by GFP and stained with anti-Disp (red in *E*) and anti-Ihog antibodies (blue in *E* and gray in *E′*). (*E′*) Note that the expression of Disp$^{AAA}$ does not cause an increase of Ihog protein levels. (*F–F′′*) Basal confocal section of an ectopic clone coexpressing IhogRFP and HhC85SN-GFP, without cholesterol and palmitic acid adducts. Note that this unlipidated form of Hh, which cannot signal, is not able to decorate cellular extensions labeled with Ihog (arrowheads in *F′* and *F′′*) as does the lipidated form (*Inset a′*).

a possible role for Ihog in Hh subcellular localization at the basolateral membrane of producing cells. Accordingly, in *ihog* mutant clones, Hh levels at the plasma membrane were reduced at the lateral and basal levels, although, interestingly, no significant reduction was evident apically (Fig. S4 *F–F′′′*) (25).

Given the localization of Ihog at the basolateral plasma membrane, we then looked at the putative interaction of Ihog with Disp and Dlp. Although mutant cells for Ihog and Boi do not have an effect on Dlp levels, we noticed that ectopic expression of Ihog increased levels of endogenous Dlp and stabilized it in membranes and cellular extensions (Fig. S5 *A* and *A′*). We additionally found that coexpression of IhogYFP and Disp revealed remarkably good colocalization along the entire filopodia length (Fig. S5 *B* and *B′*). However, the mutant form Disp$^{AAA}$ is not recruited in the basal cellular extension (Fig. S5 *C* and *C′*), as is WT Disp protein when coexpressed with Ihog protein. Furthermore, clones ectopically expressing Disp accumulate endogenous Ihog in cell membranes (Fig. 5 *D–D′′*). However, the mutant form Disp$^{AAA}$ has lost the ability to recruit Ihog protein (Fig. 5 *E* and *E′*). Taken together, these data indicate that Disp may have a more generic function in regulating vesicular trafficking and that, in addition to Hh, it may be important for subcellular localization of both Dlp and Ihog. By immunoelectron microscopy, we detected Disp and Ihog at the basolateral plasma membrane and in MVBs, where it colocalized with Hh (arrowheads in Fig. S6).

It has been described that Hh-N, HhC85S, or both (HhC85SN) are not able to signal normally in the wing imaginal disk (14, 46). We therefore tested if lipid-unmodified Hh colocalizes with Ihog in filopodia-like structures. To do so, we induced clones expressing both IhogRFP and the lipid-unmodified form of HhGFP. In noticeable contrast to what is seen with HhGFP, HhC85SN-GFP does not decorate basolateral extensions (Fig. 5 *F–F′′*, arrowheads). As previously reported (11), we observed that mutant forms of HhGFP that lacked lipid modifications are released (Fig. S3*E*) and did not accumulate in *disp*$^{-/-}$ clones (Fig. S3 *C–D′*). Taken together, these results suggest that lipid modifications of Hh protein are necessary for Disp-regulated Hh trafficking required for its release.

## Discussion

In the wing imaginal disk epithelium, as in other highly polarized cells (28, 29), two pools of Hh, apical and basolateral, are observed; however, our current work provides evidence that Hh is released and delivered to receiving cells in the A compartment following a basolateral route. We observed that the apical secreted Hh is recycled to the basolateral part of the disk epithelium, where the long-range Hh signaling is formed.

By using *shi*$^{ts1}$ mutant disks, it is possible to freeze Hh internalization and visualize on which side of the A wing disk epithelium, apical or basal, Hh gradient is being formed. Thus, we observed an extended basolateral accumulation of Hh in receiving cells, whereas, at the apical plane, Hh accumulation was only evident in the first row of A cells, indicating that the long-range Hh gradient is formed mainly basolaterally. Accordingly, Ptc accumulated in *shi*$^{ts1}$ disks equally apically and basolaterally but mainly colocalized with Hh at the basolateral sections, suggesting a specific mechanism to deliver Hh to Ptc in this surface of the disk epithelium. To analyze the mechanism of Hh release in the P cells, we noticed an apical accumulation of Hh in the producing cells in *shi*$^{ts1}$ mutant disks, which was also observed in P *shi*$^{ts1}$ clones and in Rab5$^{DN}$ ectopic clones, suggesting that the apically secreted Hh is also internalized in P cells and probably is recycling to other membranes. Accordingly, when blocking recycling endosomes (using the dominant-negative form of Rab8 or Rab4), we could detect Hh accumulation in producing cells. This Hh recycling in P cells is probably necessary to form a proper Hh gradient in the receiving cells. In agreement with the above, Hh signaling is compromised when endocytosis is blocked by expressing either Rab5$^{DN}$ or Shi$^{DN}$ in the P compartment. Interestingly, and in agreement with our results, Ayers et al. (27) suggested that apical Hh internalization in the Hh-producing cells is necessary to process or route Hh to activate the responses that require high levels of Hh. However, in contrast to our interpretation, Ayers et al. (27) also proposed that the apical Hh pool is responsible for the long-range Hh gradient formation. We believe that it is not necessary to envision two Hh gradients, an apical long-range Hh and another basolateral short-range Hh, when all responses can be produced by means of a single gradient. Because only the recycled Hh is capable of activating the high-threshold Hh targets, there is no reason to believe that this processed Hh would not be efficient enough to induce the low-threshold targets basolaterally.

Also in contrast to a previous report proposing a function for Disp in regulating the apical secretion of Hh in *Drosophila* epithelia (47), we demonstrate here that Disp is required for the basolateral release of Hh in the wing imaginal disk epithelium. The subcellular localization of Disp, and its function in the basolateral release of Hh, is in agreement with a recent report in vertebrates (48). The cellular phenotype of the loss of Disp function, such as the increase in the amount of Hh found in endocytic vesicles, which are supernumerary and disorganized, can be interpreted as

a failure in Hh trafficking that subsequently affects its proper release. In this sorting process, Hh would interact with Disp either in the recycling endosome or in MVBs. Disp, a member of the RND family of proton-driven transporters (44, 49), is likely to function only in compartments where a transmembrane proton gradient exists, such as in early and late endosomes, trans-Golgi, and MVBs. In support of this view, we showed by confocal and EM studies that Disp protein is located not only at the basolateral plasma membrane but in vesicles and MVBs, where it colocalizes with Hh. Based on the *disp*$^{-/-}$ phenotypes and the localization of Disp protein in MVBs, we propose that Disp might have a function in redirecting the apically internalized Hh toward the basal domain. Interestingly, and in agreement with the above, a form of Disp, mutant for the proton-driven transporter function (Disp$^{AAA}$), does not localize at the basolateral plasma membrane but in supernumerary cytoplasmic vesicles that do not colocalize with Hh puncta, implying that Disp$^{AAA}$ may not participate in Hh vesicular trafficking to the basolateral plasma membrane.

In noticeable contrast but also supporting the above, after freezing Hh internalization in *shi*$^{ts1}$ mutant disks, Hh accumulates apically in the first row of A compartment cells, suggesting that paracrine signaling could also occur through the apical plasma membrane. Interestingly, in P mutant cells for Dlp, Hh is able to signal to the abutting A cells but long-range signaling does not occur. A suggestive possibility is that the capacity for apical signaling is not affected in these mutant conditions; however, for long-range signaling to occur, a basolateral release implicating the coordinated actions of Dlp and Ihog together with Disp would be required. During Hh sorting in the producing cells, Disp may interact with Dlp and Ihog; in fact, the interaction of Disp with Dlp and Ihog may be important for the apical-to-basal transcytosis of these proteins, because the ectopic expression of Disp but not of mutant Disp$^{AAA}$ increases Dlp and Ihog levels at the basolateral membranes. As in *disp*$^{-/-}$ cells, *dlp*$^{-/-}$ cells in the P compartment showed an accumulation of Hh at both the apical and basolateral plasma membranes, suggesting that Dlp might cooperate with Disp during Hh release. In agreement with the proposed mechanism, transcytosis of Dlp has previously been suggested to be important for Wingless (Wg) release and spreading (45).

Although our data cannot support that the total amount of synthesized Hh has to undergo this apical-to-basal transcytosis, an intriguing question is why Hh is placed and internalized apically and then shuttled to the basolateral part of the cell. One possibility is that the newly synthesized Hh protein, because of its unusual modifications with cholesterol and palmitate, uses the apical surface, which is enriched in cholesterol and glycosphingolipids, for primarily plasma membrane localization. Alternatively, it is also possible that the apical internalization of Hh allows its interaction with Disp, glypicans, and Ihog. Therefore, Hh that reaches the apical plasma membrane needs to be internalized to recycle to the basolateral plasma membrane, where the machinery for secretion and gradient formation is found. As we have already discussed, transcytosis of Dlp and Ihog together with Hh from the apical membrane to the basolateral membrane may also occur. Cholesterol and triglycerides also undergo apical-to-basolateral transcytosis across intestinal epithelial barriers to reach the blood (50). Cholesterol and palmitic acid modifications could attribute lipid-like properties to the Hh protein, such as the ability to be anchored to the plasma membrane, and could thus affect Hh intracellular trafficking. In agreement with the above, it has been described that lipid-unmodified Hh in the wing disk epithelium is not able to form a proper Hh gradient (11, 14, 26). As previously reported (11), we observed that Hh mutant forms that lack lipid modifications are released and did not accumulate in *disp*$^{-/-}$ clones. Interestingly, we show that lipid-unmodified Hh does not colocalize with Ihog-labeled basal cell extensions, indicating that lipid modifications are necessary to interact with Disp, Dlp, and Ihog, and therefore for proper Hh trafficking from the apical to basolateral plasma membrane regulated by Disp function. Reinforcing our findings, it has been reported that *disp* (11) and *ttv* functions (51) are not required for either release or transport of lipid-unmodified Hh, strongly suggesting that Disp and glypicans are needed for the appropriate basolateral release of Hh.

Our work shows that Hh has a more complicated mechanism for release than has been previously anticipated. The finding of a basolateral route for Hh release and gradient formation will help to understand Hh interaction with different Hh pathway components, such as Disp, Dally, Dlp, Ihog, Boi, and Ptc, during the process of Hh gradient formation. Related to this issue, it is quite intriguing to find Disp, Dlp, Ihog, and Hh decorating long basal cellular extensions in disk cells expressing Ihog ectopically. Some of the long filaments labeled with IhogYFP extend up to several cell diameters and are reminiscent of the "cytonemes" described by Ramírez–Weber and Kornberg (52), with a function in the transport of morphogens. In contrast to the previously described apical cytonemes (52), the extensions we visualize are mainly found at the basal part of the disk epithelium. Interestingly, in the context of Notch signaling, basal actin-based filopodia are important for lateral inhibition between nonneighboring cells (53, 54). However, further investigation will be necessary to demonstrate the implication of cytonemes in Hh gradient formation.

## Materials and Methods

The following *Gal4* drivers were utilized in the ectopic expression experiments using the *Gal4/UAS* system (55): *hh-Gal4* (56), *AB1-Gal4* (57), *ap-Gal4* (58), and *ptc-Gal4* (59). The transgenes *actin* > *CD2* > *Gal4* (60) and *ubx* > *f+* > *Gal4, UAS-βgal* (61) were used to generate ectopic clones of the UAS lines. Transient expression of the UAS constructs using the Gal4; tub-Gal80$^{ts}$ system was accomplished by maintaining the fly crosses at 18 °C and inactivating the Gal80$^{ts}$ for 16–30 h at the restrictive temperature (29 °C).

The *pUAS*-transgenes were as follows: UAS-HhGFP (21), UAS-DlpGFP (62), UAS-Disp (11), UAS-HhC85SN-GFP, UAS-HhC85S-GFP, UAS-HhN-GFP (14), *UAS*-Dicer (Bloomington Stock Center), and UAS-Ihog (24). For the UAS-DispYFP line, YFP sequences were tagged in-frame to the N-terminal sequences of Disp cDNA. The DispYFP rescues *disp*$^{-/-}$ clones. For the UAS-IhogYFP line, UAS-IhogRFP line, and UAS-Disp$^{AAA}$-RFP, Ihog and Disp cDNAs were amplified by PCR, cloned in the entry vector pENTR/D-TOPO by directional TOPO cloning (Gateway system; Invitrogen), and introduced by recombination into the destination vectors pTWV (PUAST-VenusYFP) and pTWR (PUAST-RFP). These UAS-Ihog and UAS-Disp$^{AAA}$ fusion proteins behave like the UAS-Ihog (24) and the UAS-Disp$^{AAA}$-Myc (44). UAS-Disp$^{AAA}$-Myc transgenic fly lines were made from the mutant Disp construct described in by Ma et al. (44). For the UAS-HhCFP, the CFP sequence was tagged to Hh cDNA at a position between codons 254 (H) and 255 (V), where it does not interfere with the processing, secretion, and diffusion processes or with Hh signaling properties (21). UAS-RNAi against Dlp and Disp was obtained from the Research Institute of Molecular Pathology (IMP), Vienna Drosophila RNAi Center. The efficiency of these RNAis is shown in Fig. S4. UAS-Shi$^{DN}$ (32), UAS-Rab4DN-YFP, UAS-Rab5$^{DN}$-YFP, and UAS-Rab8$^{DN}$-YFP (34) were obtained from the Bloomington Stock Center.

**ACKNOWLEDGMENTS.** We are grateful to Tom Kornberg for critical reading of the manuscript. We thank A. Villasante and I. Sandoval for discussions and suggestions. We also thank personnel at the EM Unit of the Centro de Biología Molecular "Severo Ochoa," especially Milagros Guerra, for their skillful technical assistance. We are grateful to P. Beachy, T. Tabata, S. Eaton, R. Holmgren, M. Crozatier, and the Developmental Studies Hybridoma Bank at the University of Iowa for providing antibodies and to P. Beachy, S. Bray, K. Basler, X. Lin, H. Nakato, J. P. Vincent, the Bloomington Stock Center, and the Institute of Molecular Pathology's Vienna Drosophila RNAi Center for *Drosophila* stocks. This work was supported by Grants BFU2005-04183 and BFU2008-03320/BMC and by Consolider Program CDS 2007-00008 from the Spanish MICINN, by Marie Curie RTN FP6 (RTN 035528-2) and FP7 (ITN 238186) projects, and by an institutional grant from the Fundación Areces to I.G. It was also financially supported by fellowships awarded by the Junta para la Ampliación de Estudios-Consejo Superior de Investigaciones Cientificas program (to N.G. and A.C.), a Juan de la Cierva fellowship from the Spanish MICINN (to A.B.), a Marie Curie RTN 035528-2 FP6 contract (to E.M.), a contract from the Spanish MICINN (to L.D.), and the senior researcher Programa Amarouto from Severo Ochoa Fondation program of the Comunidad Autónoma de Madrid (G.A.).

1. Clement V, Sanchez P, de Tribolet N, Radovanovic I, Ruiz i Altaba A (2007) HEDGEHOG-GLI1 signaling regulates human glioma growth, cancer stem cell self-renewal, and tumorigenicity. *Curr Biol* 17:165–172.
2. Hochman E, Castiel A, Jacob-Hirsch J, Amariglio N, Izraeli S (2006) Molecular pathways regulating pro-migratory effects of Hedgehog signaling. *J Biol Chem* 281:33860–33870.
3. Charron F, Stein E, Jeong J, McMahon AP, Tessier-Lavigne M (2003) The morphogen sonic hedgehog is an axonal chemoattractant that collaborates with netrin-1 in midline axon guidance. *Cell* 113:11–23.
4. Pasca di Magliano M, Hebrok M (2003) Hedgehog signalling in cancer formation and maintenance. *Nat Rev Cancer* 3:903–911.
5. Ingham PW, Placzek M (2006) Orchestrating ontogenesis: Variations on a theme by sonic hedgehog. *Nat Rev Genet* 7:841–850.
6. Garcia-Bellido A, Ripoll P, Morata G (1973) Developmental compartmentalisation of the wing disk of Drosophila. *Nat New Biol* 245:251–253.
7. Kornberg TB, Guha A (2007) Understanding morphogen gradients: A problem of dispersion and containment. *Curr Opin Genet Dev* 17:264–271.
8. Mann RK, Beachy PA (2004) Novel lipid modifications of secreted protein signals. *Annu Rev Biochem* 73:891–923.
9. Peters C, Wolf A, Wagner M, Kuhlmann J, Waldmann H (2004) The cholesterol membrane anchor of the Hedgehog protein confers stable membrane association to lipid-modified proteins. *Proc Natl Acad Sci USA* 101:8531–8536.
10. Amanai K, Jiang J (2001) Distinct roles of Central missing and Dispatched in sending the Hedgehog signal. *Development* 128:5119–5127.
11. Burke R, et al. (1999) Dispatched, a novel sterol-sensing domain protein dedicated to the release of cholesterol-modified hedgehog from signaling cells. *Cell* 99:803–815.
12. Han C, et al. (2004) Distinct and collaborative roles of Drosophila EXT family proteins in morphogen signalling and gradient formation. *Development* 131:1563–1575.
13. Takei Y, Ozawa Y, Sato M, Watanabe A, Tabata T (2004) Three Drosophila EXT genes shape morphogen gradients through synthesis of heparan sulfate proteoglycans. *Development* 131:73–82.
14. Callejo A, Torroja C, Quijada L, Guerrero I (2006) Hedgehog lipid modifications are required for Hedgehog stabilization in the extracellular matrix. *Development* 133: 471–483.
15. Eugster C, Panáková D, Mahmoud A, Eaton S (2007) Lipoprotein-heparan sulfate interactions in the Hh pathway. *Dev Cell* 13:57–71.
16. Lin X (2004) Functions of heparan sulfate proteoglycans in cell signaling during development. *Development* 131:6009–6021.
17. Desbordes SC, Sanson B (2003) The glypican Dally-like is required for Hedgehog signalling in the embryonic epidermis of Drosophila. *Development* 130:6245–6255.
18. Lum L, et al. (2003) Identification of Hedgehog pathway components by RNAi in Drosophila cultured cells. *Science* 299:2039–2045.
19. Chen Y, Struhl G (1996) Dual roles for patched in sequestering and transducing Hedgehog. *Cell* 87:553–563.
20. Casali A, Struhl G (2004) Reading the Hedgehog morphogen gradient by measuring the ratio of bound to unbound Patched protein. *Nature* 431:76–80.
21. Torroja C, Gorfinkiel N, Guerrero I (2004) Patched controls the Hedgehog gradient by endocytosis in a dynamin-dependent manner, but this internalization does not play a major role in signal transduction. *Development* 131:2395–2408.
22. Lum L, Beachy PA (2004) The Hedgehog response network: Sensors, switches, and routers. *Science* 304:1755–1759.
23. Yao S, Lum L, Beachy P (2006) The ihog cell-surface proteins bind Hedgehog and mediate pathway activation. *Cell* 125:343–357.
24. Zheng X, Mann RK, Sever N, Beachy PA (2010) Genetic and biochemical definition of the Hedgehog receptor. *Genes Dev* 24:57–71.
25. Yan D, et al. (2010) The cell-surface proteins Dally-like and Ihog differentially regulate Hedgehog signaling strength and range during development. *Development* 137: 2033–2044.
26. Gallet A, Ruel L, Staccini-Lavenant L, Thérond PP (2006) Cholesterol modification is necessary for controlled planar long-range activity of Hedgehog in Drosophila epithelia. *Development* 133:407–418.
27. Ayers KL, Gallet A, Staccini-Lavenant L, Thérond PP (2010) The long-range activity of Hedgehog is regulated in the apical extracellular space by the glypican Dally and the hydrolase Notum. *Dev Cell* 18:605–620.
28. Danesin C, et al. (2006) Ventral neural progenitors switch toward an oligodendroglial fate in response to increased Sonic hedgehog (Shh) activity: Involvement of Sulfatase 1 in modulating Shh signaling in the ventral spinal cord. *J Neurosci* 26:5037–5048.
29. Chamberlain CE, Jeong J, Guo C, Allen BL, McMahon AP (2008) Notochord-derived Shh concentrates in close association with the apically positioned basal body in neural target cells and forms a dynamic gradient during neural patterning. *Development* 135:1097–1106.
30. Tabata T, Kornberg TB (1994) Hedgehog is a signaling protein with a key role in patterning Drosophila imaginal discs. *Cell* 76:89–102.
31. van der Bliek AM (1999) Is dynamin a regular motor or a master regulator? *Trends Cell Biol* 9:253–254.
32. Moline MM, Southern C, Bejsovec A (1999) Directionality of wingless protein transport influences epidermal patterning in the Drosophila embryo. *Development* 126:4375–4384.
33. Stenmark H, et al. (1994) Inhibition of rab5 GTPase activity stimulates membrane fusion in endocytosis. *EMBO J* 13:1287–1296.
34. Zhang J, et al. (2007) Thirty-one flavors of Drosophila rab proteins. *Genetics* 176: 1307–1322.
35. Sevrioukov EA, He JP, Moghrabi N, Sunio A, Krämer H (1999) A role for the deep orange and carnation eye color genes in lysosomal delivery in Drosophila. *Mol Cell* 4: 479–486.
36. Ikonen E (2008) Cellular cholesterol trafficking and compartmentalization. *Nat Rev Mol Cell Biol* 9:125–138.
37. Linder MD, et al. (2007) Rab8-dependent recycling promotes endosomal cholesterol removal in normal and sphingolipidosis cells. *Mol Biol Cell* 18:47–56.
38. Hoekstra D, Tyteca D, van IJzendoorn SC (2004) The subapical compartment: A traffic center in membrane polarity development. *J Cell Sci* 117:2183–2192.
39. Seachrist JL, Anborgh PH, Ferguson SS (2000) beta 2-adrenergic receptor internalization, endosomal sorting, and plasma membrane recycling are regulated by rab GTPases. *J Biol Chem* 275:27221–27228.
40. Lazzarino DA, Blier P, Mellman I (1998) The monomeric guanosine triphosphatase rab4 controls an essential step on the pathway of receptor-mediated antigen processing in B cells. *J Exp Med* 188:1769–1774.
41. Vervoort M, Crozatier M, Valle D, Vincent A (1999) The COE transcription factor Collier is a mediator of short-range Hedgehog-induced patterning of the Drosophila wing. *Curr Biol* 9:632–639.
42. Kawakami T, et al. (2002) Mouse dispatched mutants fail to distribute hedgehog proteins and are defective in hedgehog signaling. *Development* 129:5753–5765.
43. Tian H, Jeong J, Harfe BD, Tabin CJ, McMahon AP (2005) Mouse Disp1 is required in sonic hedgehog-expressing cells for paracrine activity of the cholesterol-modified ligand. *Development* 132:133–142.
44. Ma Y, et al. (2002) Hedgehog-mediated patterning of the mammalian embryo requires transporter-like function of dispatched. *Cell* 111:63–75.
45. Gallet A, Staccini-Lavenant L, Thérond PP (2008) Cellular trafficking of the glypican Dally-like is required for full-strength Hedgehog signaling and wingless transcytosis. *Dev Cell* 14:712–725.
46. Lee JD, Treisman JE (2001) Sightless has homology to transmembrane acyltransferases and is required to generate active Hedgehog protein. *Curr Biol* 11:1147–1152.
47. Gallet A, Rodriguez R, Ruel L, Therond PP (2003) Cholesterol modification of hedgehog is required for trafficking and movement, revealing an asymmetric cellular response to hedgehog. *Dev Cell* 4:191–204.
48. Etheridge LA, Crawford TQ, Zhang S, Roelink H (2010) Evidence for a role of vertebrate Disp1 in long-range Shh signaling. *Development* 137:133–140.
49. Tseng TT, et al. (1999) The RND permease superfamily: An ancient, ubiquitous and diverse family that includes human disease and development proteins. *J Mol Microbiol Biotechnol* 1:107–125.
50. Roger E, Lagarce F, Garcion E, Benoit JP (2009) Lipid nanocarriers improve paclitaxel transport throughout human intestinal epithelial cells by using vesicle-mediated transcytosis. *J Control Release* 140:174–181.
51. The I, Bellaiche Y, Perrimon N (1999) Hedgehog movement is regulated through tout velu-dependent synthesis of a heparan sulfate proteoglycan. *Mol Cell* 4:633–639.
52. Ramírez-Weber FA, Kornberg TB (1999) Cytonemes: Cellular processes that project to the principal signaling center in Drosophila imaginal discs. *Cell* 97:599–607.
53. De Joussineau C, et al. (2003) Delta-promoted filopodia mediate long-range lateral inhibition in Drosophila. *Nature* 426:555–559.
54. Cohen M, Georgiou M, Stevenson NL, Miodownik M, Baum B (2010) Dynamic filopodia transmit intermittent Delta-Notch signaling to drive pattern refinement during lateral inhibition. *Dev Cell* 19:78–89.
55. Brand AH, Perrimon N (1993) Targeted gene expression as a means of altering cell fates and generating dominant phenotypes. *Development* 118:401–415.
56. Tanimoto H, Itoh S, ten Dijke P, Tabata T (2000) Hedgehog creates a gradient of DPP activity in Drosophila wing imaginal discs. *Mol Cell* 5:59–71.
57. Munro S, Freeman M (2000) The notch signalling regulator fringe acts in the Golgi apparatus and requires the glycosyltransferase signature motif DXD. *Curr Biol* 10: 813–820.
58. Calleja M, Moreno E, Pelaz S, Morata G (1996) Visualization of gene expression in living adult Drosophila. *Science* 274:252–255.
59. Hinz U, Giebel B, Campos-Ortega JA (1994) The basic-helix-loop-helix domain of Drosophila lethal of scute protein is sufficient for proneural function and activates neurogenic genes. *Cell* 76:77–87.
60. Pignoni F, Zipursky SL (1997) Induction of Drosophila eye development by decapentaplegic. *Development* 124:271–278.
61. de Celis JF, Tyler DM, de Celis J, Bray SJ (1998) Notch signalling mediates segmentation of the Drosophila leg. *Development* 125:4617–4626.
62. Han C, Belenkaya TY, Wang B, Lin X (2004) Drosophila glypicans control the cell-to-cell movement of Hedgehog by a dynamin-independent process. *Development* 131: 601–611.